Sensors and Actuators B 140 (2009) 623–628

Contents lists available at ScienceDirect

Sensors and Actuators B: Chemical

journal homepage: www.elsevier.com/locate/snb

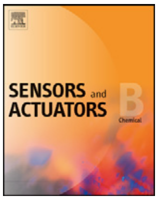

Nanoplates of α-$SnWO_4$ and SnW_3O_9 prepared via a facile hydrothermal method and their gas-sensing property

Hui Dong, Zhaohui Li*, Zhengxin Ding, Haibo Pan, Xuxu Wang, Xianzhi Fu*

Research Institute of Photocatalysis, Fuzhou University, State Key Laboratory Breeding Base of Photocatalysis, Fuzhou 350002, PR China

ARTICLE INFO

Article history:
Received 19 March 2009
Received in revised form 2 May 2009
Accepted 11 May 2009
Available online 19 May 2009

Keywords:
$SnWO_4$
SnW_3O_9
Nanoplate
Hydrothermal
Gas-sensing

ABSTRACT

Nanoplates of α-$SnWO_4$ and SnW_3O_9 were selectively synthesized in large scale via a facile hydrothermal reaction method. The final products obtained were dependent on the reaction pH and the molar ratio of W^{6+} to Sn^{2+} in the precursors. The as-prepared nanoplates of α-$SnWO_4$ and SnW_3O_9 were characterized by X-ray powder diffraction (XRD), N_2-sorption BET surface area, transmission electron microscopy (TEM), high-resolution transmission electron microscopy (HRTEM) and X-ray photoelectron spectroscopy (XPS). The XPS results showed that Sn exists in divalent form (Sn^{2+}) in SnW_3O_9 as well as in α-$SnWO_4$. The gas-sensing performances of the as-prepared α-$SnWO_4$ and SnW_3O_9 toward H_2S and H_2 were investigated. The hydrothermal prepared α-$SnWO_4$ showed higher response toward H_2 than that prepared via a solid-state reaction due to the high specific surface area. The gas-sensing property toward H_2S as well as H_2 over SnW_3O_9 was for the first time reported. As compared to α-$SnWO_4$, SnW_3O_9 exhibits higher response toward H_2S and its higher response can be well explained by the existence of the multivalent W (W^{6+}/W^{4+}) in SnW_3O_9.

1. Introduction

Since both SnO_2 and WO_3 are well-known materials in the semiconductor gas-sensor field and have found applications in commercial sensor devices, the studies on the gas-sensing property of ternary Sn–W–O systems have also attracted a lot of interest [1–3]. Most already reported Sn-based gas-sensing semiconductors contain Sn^{4+} as in the case of SnO_2 [4–6]. The inclusions of both Sn^{4+} and Sn^{2+} have also been reported in some Sn–W–O gas-sensing semiconductors. For example, Solis and Lantto [3] reported the gas-sensing property of Sn_xWO_{3+x} with the atomic ratio x between 1.25 and 2.5. The only reported Sn^{2+}-based gas-sensing semiconductor is α-$SnWO_4$. Since tin in the divalent form may enable an electron transfer between the Sn^{2+} lattice ions at the surface and surface adsorbates, the developments of other Sn–W–O gas-sensing materials with Sn in divalent state would be interesting.

α-$SnWO_4$ is an n-type semiconductor with an orthorhombic crystal structure and both Sn and W atoms have distorted octahedral oxygen coordinations [1,2]. Traditional methods in the preparations of the ternary Sn–W–O mixed oxides, including α-$SnWO_4$, are solid-state reactions [3,7,8] or the direct redox reaction between metal Sn and the tungstenic acid [9]. Since Sn^{2+} can be easily oxidized to Sn^{4+}, these reactions have to be carried out under N_2 atmosphere. The other disadvantage of these reaction methods is the difficulty in the preparations of nanocrystalline products with small particle size and high surface area. The as-obtained products are therefore not favorable for the applications in the gas-sensor field since a high “surface accessibility” is crucial in obtaining a high sensitivity of the semiconductor material [10–12]. According to the generally accepted theory, the gas sensitivity of a semiconductor material is generated by the gas–solid interactions, i.e., the adsorption/desorption and reactions on the semiconductor surface [13]. Therefore nanocrystalline semiconductor materials with small particle sizes and high active surface area are expected to exhibit superior gas-response property to their bulk counterpart since they can provide more active surface for the adsorbates [14–16]. Although sometimes the instability of the sensitivity is observed due to the evolution of the fine microstructure during the working of the sensor at high temperature, the application of the nanomaterials for gas-sensing still attracted much recent interest. For example, a recent report showed that the sensor made of hierarchical Cu_2O microspheres with hollow and multilayered configuration exhibited much higher gas-sensing property than bulk Cu_2O [15].

The applications of low temperature hydrothermal method in the preparations of pure crystalline nanomaterials with small particle size, narrow grain size-distribution and large specific surface area without high temperature treatment have been well documented. To make the hydrothermal method more attractive is that

---

* Corresponding authors. Tel.: +86 591 83779105; fax: +86 591 83779105.
E-mail addresses: zhaohuili1969@yahoo.com (Z. Li), xzfu@fzu.edu.cn (X. Fu).

0925-4005/$ – see front matter © 2009 Elsevier B.V. All rights reserved.
doi:10.1016/j.snb.2009.05.010

it can give products with tunable morphology and particle size by simply adjusting the reaction temperature, time and reaction pH as well as using the additives [17].

Herein, we report the selective syntheses of nanoplates of α-$SnWO_4$ and SnW_3O_9 in large scale via a facile low temperature hydrothermal route. The reaction pH and the molar ratio of W^{6+} to Sn^{2+} in the precursors played important roles in the final products obtained. Although the hydrothermal method has been applied in the preparations of many tungstates [18–20], to the best of our knowledge, it has never been reported in the preparations of ternary Sn–W–O mixed oxides. The gas-sensing performances of the as-prepared α-$SnWO_4$ and SnW_3O_9 toward H_2S and H_2 were also investigated. SnW_3O_9 represents another ternary Sn(II)–W–O semiconductor which shows gas-sensing property. Our result also revealed that the hydrothermal prepared α-$SnWO_4$ showed higher sensitivity toward H_2 than that prepared via a solid-state reaction.

2. Experimental

2.1. Syntheses

Nanocrystalline α-$SnWO_4$ and SnW_3O_9 were prepared by the hydrothermal method. All of the reactants and solvents were analytical grade and were used without further purifications.

In a typical procedure for the preparation of α-$SnWO_4$, $SnCl_2{\cdot}2H_2O$ (1.128 g, 5 mmol), $(NH_4)_5H_5[H_2(WO_4)_6]{\cdot}H_2O$ (1.335 g, 0.833 mmol) (molar ratio of Sn^{2+} to W^{6+} at 1:1) were added to 65 mL aqueous solution. The pH of the resulting mixture was adjusted to 1, 3, 5, 7, 9 and 11 with sodium hydrate solution ($2\,mol\,L^{-1}$) under vigorous stirring. The resulting suspension was transferred to a 100 mL Teflon-lined stainless steel autoclave and sealed tightly. The autoclaves were kept at 200 °C for 48 h. After cooling to room temperature, the precipitate was collected, washed with distilled water and then dried in air at 80 °C. The procedure for the preparation of pure SnW_3O_9 is similar to that of α-$SnWO_4$ except that the molar ratio of Sn^{2+} to W^{6+} is 1:2 and the pH value is lower than 1.

For comparison, bulk α-$SnWO_4$ sample was prepared from SnO and WO_3 using a conventional solid-state synthesis route [3]. To prevent the oxidation of Sn^{2+} to Sn^{4+}, SnO and WO_3 was heated in an argon atmosphere at 600 °C for 15 h to obtain the sample.

2.2. Characterizations

X-ray diffraction (XRD) patterns were collected on a Bruker D8 Advance X-ray diffractometer with CuK_α radiation. The accelerating voltage and the applied current were 40 kV and 40 mA, respectively. Data were recorded at a scanning rate of $0.02^\circ\,s^{-1}$ in the 2θ range of 10–70°. It was used to identify the phase present and their crystallite size. The crystallite size was calculated from X-ray line broadening analysis by Scherer equation: $D = 0.89\lambda/\beta\cos\theta$, where D is the crystal size in nm, λ is the CuK_α wavelength (0.15406 nm), β is the half-width of the peak in rad, and θ is the corresponding diffraction angle. The Brunauer–Emmett–Teller (BET) surface area was measured with an ASAP2020M (Micromeritics Instrument Corp.). The transmission electron microscopy (TEM) and high-resolution transmission electron microscopy (HRTEM) images were measured by JEOL model JEM 2010 EX instrument at the accelerating voltage of 200 kV. The powder particles were supported on a carbon film coated on a 3 mm diameter fine-mesh copper grid. A suspension in ethanol was sonicated and a drop was dripped on the support film. X-ray photoelectron spectroscopy (XPS) measurements were carried out using a VG Scientific ESCA Lab Mark II spectrometer equipped with two ultra-high vacuum 6 (UHV) chambers. All binding energies were referenced to the C 1s peak of the surface adventitious carbon at 284.8 eV.

2.3. Gas-sensing property measurements

The sensor structure and the testing principle were similar to that reported previously [10,11,21]. The electrode for measurement was composed of a pair of four-fingered gold electrodes of 120 μm width and 40 μm spacing between fingers on an alumina substrate. The overlap distance of the fingers was 400 μm, and a Ni–Cr heater (37 Ω) was made on the opposing face of the substrate. The thick film was coated with a layer of sensor materials of about 10 μm thick. After drying at 150 °C for 2 h in air to improve the stability, the electrical contact was made through connecting the four platinum wires with the instrument base by silver paste. During the measurement, the sensors were hosted in a closed plastic tube equipped with appropriate inlets and outlets for gas flow. A given amount of gas such as H_2S or H_2 was injected into the chamber by a micro-injector. The resistance of a sensitive material is measured in air (R_{air}) and in air–gas mixtures (R_{gas}) under the same operating current. The gas response magnitude (S) was defined as the ratio of R_{air} to R_{gas} ($S = R_{air}/R_{gas}$).

3. Results and discussion

3.1. Syntheses

The pH value plays an important role in controlling the composition of the final products. Fig. 1 shows the XRD patterns for the products obtained from the hydrothermal treatment of the precursors with a 1:1 molar ratio of W^{6+} to Sn^{2+} at 200 °C for 48 h under different pH values. It is observed that pure phase of α-$SnWO_4$ (JCPDS no. 29-1354) can only be obtained at a neutral pH value (from 6 to 9) although the formation of the phase of α-$SnWO_4$ starts at pH of 2. The products obtained in the acidic condition (pH from 2 to 5) are a mixture of α-$SnWO_4$, SnW_3O_9 (JCPDS no. 86-628) and SnO_2. With pH decreasing to 1, the phase of α-$SnWO_4$ cannot be obtained and the product obtained is a mixture of SnW_3O_9 and SnO_2. With pH increasing to basic condition, a mixture of SnO_2 and SnO can be obtained.

The molar ratio of W^{6+} to Sn^{2+} also plays an important role in the final product. Fig. 2 shows the representative XRD patterns of the products obtained when treated hydrothermally at 200 °C at a pH value lower than 1 under different molar ratio of W^{6+} to Sn^{2+}. It is found that pure SnW_3O_9 can only be obtained when the molar ratio of W^{6+} to Sn^{2+} is 2:1. A lower molar ratio of W^{6+} to Sn^{2+} (<2:1) only gives a mixture of SnO_2 and SnW_3O_9. It is not strange that pure

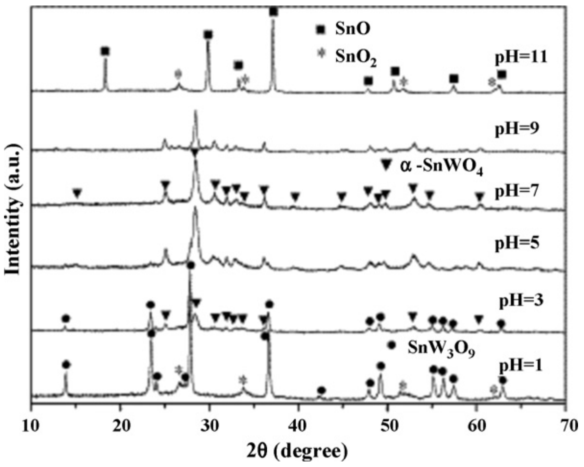

Fig. 1. XRD patterns of the samples prepared at 200 °C for 48 h with different pH values, (a) pH 1; (b) pH 3; (c) pH 5; (d) pH 7; (e) pH 9; (f) pH 11. (●) SnW_3O_9; (*) SnO_2; (▼) α-$SnWO_4$; (■) SnO.